Neuron specific reduction in CuZnSOD is not sufficient to initiate a full sarcopenia phenotype

Kavithalakshmi Sataranatarajan[1*], Rizwan Qaisar[1*], Carol Davis[4], Giorgos K Sakellariou[3], Aphrodite Vasilaki[3], Yiqiang Zhang[6], Yuhong Liu[7], Shylesh Bhaskaran[1], Anne McArdle[3], Malcolm Jackson[3], Susan V. Brooks[4], Arlan Richardson[2, 5] and Holly Van Remmen[1, 2]

* denotes equal contribution by these authors

[1] Free Radical Biology and Aging Program, Oklahoma Medical Research Foundation, Oklahoma City, OK 73104.

[2] Oklahoma VA Medical Center, Oklahoma City, OK 73104.

[3]Liverpool -MRC Arthritis Research UK Centre for Integrated research into Musculoskeletal Ageing (CIMA), Department of Musculoskeletal Biology, Institute of Ageing and Chronic Disease, University of Liverpool, UK.

[4]Department of Molecular and Integrative Physiology, University of Michigan

[5] Reynolds Oklahoma Center on Aging, University of Oklahoma Health Sciences Center and Oklahoma City VA Medical Center, Oklahoma, OK, USA

[6] Department of Biochemistry, UT Southwestern Medical Center, Dallas, TX,USA

[7] The Sam and Ann Barshop Institute for Longevity and Aging Studies, The University of Texas Health Science Center at San Antonio, San Antonio, TX, USA

Keywords: CuZnSOD, oxidative stress, neuromuscular junction, muscle atrophy, sarcopenia

Corresponding Author
Holly Van Remmen, PhD
Free Radical Biology and Aging Research Program,
Oklahoma Medical Research Foundation,
825 N.E. 13th Street,
Oklahoma City,
OK 73104.
Phone: (405) 271-2520
Fax: (405) 271-3470
E-mail: holly-vanremmen@omrf.org

Highlights

The sarcopenia phenotype of mice lacking CuZnSOD in all tissues is not recapitulated in mice with a neuron specific deletion of CuZnSOD (n*Sod1*KO mice)

Neuronal loss of CuZnSOD reduces force generation to a small extent, but mass is not reduced in the gastrocnemius muscle in 20 month old mice, a muscle that is highly sensitive to age related loss of muscle mass and strength

Loss of CuZnSOD in neuronal tissue alters NMJ morphology and induces moderately markers of muscle denervation; however, it does not initiate neuromuscular junction degeneration, loss of innervation or increases in oxidative stress or mitochondrial generation of ROS.

Our data support the concept that deficits in either the motor neuron or muscle alone are not sufficient to initiate a full sarcopenic phenotype.

Abstract.

Our previous studies showed that adult (8 month) mice lacking CuZn-superoxide dismutase (CuZnSOD, *Sod1*KO mice) have neuromuscular changes resulting in dramatic accelerated muscle atrophy and weakness that mimics age-related sarcopenia. We have further shown that loss of CuZnSOD targeted to skeletal muscle alone results in only mild weakness and no muscle atrophy. In this study we targeted deletion of CuZnSOD specifically to neurons (n*Sod1*KO mice) and determined the effect on muscle mass and weakness. The n*Sod1*KO mice show a significant loss of CuZnSOD activity and protein level in brain and spinal cord but not in muscle tissue. The masses of the gastrocnemius, tibialis anterior and extensor digitorum longus (EDL) muscles were not reduced in n*Sod1*KO compared to wild type mice, even at 20 months of age, although the quadriceps and soleus muscles showed small but significant reductions in mass in the n*Sod1*KO mice. Maximum isometric specific force was reduced 8% to 10% in the gastrocnemius and EDL muscle of n*Sod1*KO mice, while soleus was not affected. Muscle mitochondrial ROS generation and oxidative stress measured by levels of reactive oxygen/nitrogen species (RONS) regulatory enzymes, protein nitration and F_2-isoprostane levels were not increased in muscle from the n*Sod1*KO mice. Although we did not find evidence of denervation in the nSOD1KO mice, neuromuscular junction morphology was altered and the expression of genes associated with denervation (acetylcholine receptor subunit alpha (AChRα) and the transcription factors Runx1 and GADD45α) was increased, supporting a role for neuronal loss of CuZnSOD initiating alterations at the neuromuscular junction. These results and our previous studies support the concept that deficits in either the motor neuron or muscle alone are not sufficient to initiate a full sarcopenic phenotype and that deficits in both tissues are required to recapitulate the loss of muscle observed in *Sod1*KO mice.

Introduction

Our previous studies have provided significant insight into potential mechanisms of sarcopenia using mice that lack CuZn-superoxide dismutase (CuZnSOD), i.e., *Sod1*KO mice, as a model of age-related muscle atrophy. Although indistinguishable from wild type mice at birth, by 5-8 months of age, gastrocnemius muscles of *Sod1*KO mice display significant reductions in mass and function that progress through adulthood, such that by 20 months of age *Sod1*KO mice resemble 30-month-old wild type mice (Muller et al., 2006, Jang et al., 2010, Larkin et al., 2011). In addition, both *Sod1*KO mice and old wild type mice exhibit profound alterations in neuromuscular innervation in conjunction with the initiation of skeletal muscle atrophy (Jang et al., 2010). Post-synaptic endplates are severely disrupted, the number of acetylcholine receptors (AChRs) is reduced and the receptors are significantly fragmented. Finally, mitochondrial function is reduced and mitochondrial ROS generation is elevated in both adult *Sod1*KO mice and old wild type mice. Overall, our findings in the *Sod1*KO mice point to the significance of neuromuscular interaction in maintenance of mitochondrial function and muscle mass and suggest that disruption of the neuromuscular junction (NMJ) might be a trigger for declines in muscle mass and function during aging.

Because muscle and motor neurons are integrally related by structure and function, the question has always arisen as to the relative roles of these two tissues in the mechanism responsible for muscle atrophy. Similar questions have been raised in the field of ALS and other neuromuscular diseases in which muscle atrophy and weakness are a predominant phenotype. The observation that *Sod1*KO mice replicate the sarcopenia phenotype observed in old wild type mice provides us with the ability to use genetic approaches to dissect out the role of the motor neuron and muscle in sarcopenia and to begin identifying key pathways in these tissues that are critical in the loss in muscle mass and function. Our first study showed that replacing CuZnSOD specifically in the motor neurons in *Sod1*KO mice (nSOD1-Tg/*Sod1*KO mice) prevented muscle atrophy and weakness, as well as the NMJ degeneration associated with loss of mass and function. These data suggested that motor neuron deficits resulting from oxidized redox status are a key initiating event in sarcopenia in the *Sod1*KO mice (Sakellariou et al., 2014). In contrast, deleting *Sod1* specifically in skeletal muscle (m*Sod1*KO mice) had no effect on either muscle atrophy or NMJ degeneration (Zhang et al., 2013a), demonstrating that loss of *Sod1* in muscle alone is not sufficient to generate atrophy. Based on our experiments with the nSOD1-Tg/*Sod1*KO and m*Sod1*KO mice, we speculated that the loss of *Sod1* in the motor neuron was the critical feature contributing to the sarcopenia observed in the whole body Sod1 mice. Thus, we hypothesized that neuronal specific *Sod1*KO (n*Sod1*KO) mice would recapitulate the phenotype of the *Sod1*KO mice. To test this hypothesis, we

generated a neuronal specific knockout mouse using our *Sod1*-floxed mouse crossed to transgenic mice expressing Cre recombinase driven by the nestin promoter (nestin-Cre transgenic mice) and compared n*Sod1*KO and wild type mice for muscle atrophy and weakness, as well as a number of parameters that we had previously measured in the *Sod1*KO mice, including muscle properties such as fiber diameter and myonuclear domain, oxidative stress and markers of altered redox, changes in acetyl choline receptor morphology and markers of denervation. Contrary to our hypothesis, our results show that loss of neuronal CuZnSOD was not sufficient to induce muscle atrophy and weakness that is observed in the *Sod1*KO mice.

Materials and Methods

Generation of neuron-specific *Sod1*-knockout (n*Sod1*KO) mice. Details of the generation of the *Sod1*$^{flox/flox}$ mice was reported in our earlier publication (Zhang et al., 2013). To generate nSod1KO mice, *Sod1*$^{flox/flox}$ mice were bred with a mouse strain that expresses Cre recombinase under the control of the nestin promotor [(B6.Cg(SJL)-Tg(Nes-cre)1Kln/J)] that we obtained from Jackson laboratory (Bar Harbor, ME,USA). Mice were maintained on a 12-hr dark/light cycle and provided with food and water ad libitum. At sacrifice, mice were euthanized by CO_2 inhalation and tissues were immediately excised and weighed. All the tissues, except those used for immunostaining, were snap frozen and stored at −80°C. All animal protocols were consistent with The Guide for the Care and Use of Laboratory Animals and approved by the Institutional Animal Care and Use Committee at Oklahoma Medical Research Foundation (OKC, OK, USA).

Measurement of CuZnSOD and MnSOD activity. CuZnSOD and MnSOD activity in brain, spinal cord and muscle were determined using native gels as described (Van Remmen et al., 1999).

CuZnSOD immunoblot analysis. Equal amounts of protein from brain, spinal cord, gastrocnemius and quadriceps muscle were resolved by SDS-PAGE and transferred to PVDF membrane. The membranes were blocked and probed with CuZnSOD (Enzo Life Sciences, Inc. Farmingdale, NY, USA) and GAPDH (Sigma, St. Louis, MO, USA) antibodies overnight at 4 C. Membranes were washed extensively and incubated with secondary antibodies linked to horseradish peroxidase (Santa Cruz Biotechnology, Dallas, TX, USA). Proteins were visualized using enhanced chemiluminescence reagent and signal intensities were quantified using Image J 1.45b software (developed by Wayne Rasband, National Institute of Health, Bethesda, MD)

Western blotting of RONS proteins in skeletal muscle. Muscles were ground in a motor and pestle under liquid nitrogen and frozen muscle powder was placed into RIPA buffer containing 50 mM Tris (pH 7.4), 150 mM NaCl, and protease inhibitors. Samples were homogenized on ice and centrifuged at 10.000g for 10min at 4^{o}C. Protein content of samples was determined using the bicinchoninic acid method (Sigma-Aldrich, Poole, UK). For assessment of specific proteins in muscle, 20µg of total protein was applied to a 4-20% mini-PROTEAN TGX precast gel with a 4% stacking gel (Biorad Laboratories Ltd, Hemel Hempstead, UK). The separated proteins were transferred onto nitrocellulose membranes by western blotting. Membranes were probed using antibodies against MnSOD (SOD2), (Stressgen Inc., UK), eNOS, iNOS, PRXV, and GAPDH (Abcam, Cambridge, UK). Horseradish peroxidase conjugated anti-rabbit IgG or anti-mouse

IgG, (Cell Signalling, Hitchin, UK) was used as secondary antibody. Peroxidase activity was detected using an ECL Plus substrate (Amersham International Cardiff, UK), and band intensities were analysed using Quantity One Software (Biorad Laboratories Ltd). The specificity of the bands was identified in comparison with a sample that had not been exposed to the primary antibody and the molecular weight was determined by using molecular weight markers. All protein contents were normalized to the GAPDH content of the same sample.

Analyses of the 3-nitrotyrosine (3-NT) content of muscle proteins. Total cellular protein was isolated and 20μg was separated by SDS-PAGE followed by western blotting as describe above. The separated proteins were transferred onto polyvinylidene difluoride (PVDF) membranes. The content of 3-NT was analysed by using a rabbit monoclonal antibody (Cell Biolabs, San Diego, USA), as per the manufacturer's instructions. Bands were visualized and densitometric quantification was undertaken using Quantity One Software (Biorad Laboratories Ltd).

Analysis of F_2-isoprostanes. Levels of F_2-isoprostanes in quadriceps muscle was measured as decribed (Ward et al, 2005, Zhang et al., 2013). Briefly, 200mg of tissue was homogenized in 10 ml of ice-cold Folch solution ($CHCl_3$: MeOH, 2:1) containing butylated hydroxytoluene (BHT). The mixture was incubated at room temperature for 30min. 2 ml of 0.9% NaCl was added and mixed well. The homogenate was centrifuged at 3000 × g for 5 minutes at 4°C. The aqueous layer was discarded while the organic layer was secured and evaporated to dryness under N_2 at 37°C. Esterified F_2-isoprostanes were measured using gas chromatography-mass spectrometry. The level of F_2-isoprostanes in muscle tissues was expressed as nanograms of 8-Iso-$PGF_{2\alpha}$, per gram of muscle tissue.

Real-time PCR. Total RNA was extracted from the gastrocnemius and quadriceps of the wild type and nSod1KO mice using TRIzol reagent (Life Technologies, Grand Island, NY, USA). RNA purity and yield were determined by measuring the absorbance at 260 and 280nm. cDNA were prepared from 1ug of the total RNA using iScript™ cDNA Synthesis kit (Bio-Rad, Hercules, CA, USA). 2.5ng of cDNA samples were amplified using fast SYBR green master mix and primers for AChRα, Musk, Rapsyn, Runx1, GADD45a and 18S (Applied Biosystems, Grand Island, NY, USA). The data were analyzed using the ΔΔ*Ct* method.

Contractile Force. Mice were anesthetized by intraperitoneal injection of Avertin (tribromoethanol, 250 mg/kg) supplemented to maintain an adequate level of anesthesia during all procedures. Gastrocnemius muscle contractile properties were measured in situ, as described by Larkin et al. (2011). Anesthetized mice were placed on a platform warmed to maintain body temperature at 37°C. The gastrocnemius

muscle was isolated from surrounding tissues and the distal tendon was securely tied to the lever arm of a servomotor (model 6650LR, Cambridge Technology). The knee and foot were clamped to the platform. A continual drip of saline warmed to 37°C was applied to the gastrocnemius muscle to maintain its temperature. The muscle was activated by stimulation of the tibial nerve. With the muscle held at optimal length (L_o), 300-ms trains of stimulus pulses were applied at increasing stimulation frequencies until the maximum isometric tetanic force (P_o) was achieved. Contractile properties were measured for extensor digitorum longus and soleus muscles in vitro as described by Brooks and Faulkner (1988). Muscles were placed in a horizontal bath containing buffered mammalian Ringer solution maintained at 25°C and tied to a force transducer (model BG-50, Kulite Semiconductor Products, Leonia, NJ) and a servomotor (model 305B, Aurora Scientific, Aurora, ON). Muscles were stimulated by platinum plate electrodes connected to a high-power biphasic current stimulator (model 701B, Aurora Scientific). Muscles were held at L_o and subjected to trains of pulses of 300 ms duration for EDL muscles and 900 ms for soleus muscles. Stimulus frequency was increased until the P_o was achieved.

After muscles were removed, deeply anesthetized mice were euthanized by pneumothorax and removal of a vital organ. Muscles were trimmed of their tendons, blotted and weighed. Fiber lengths (L_f) were estimated by multiplying L_o by previously determined L_f-to-L_o ratios (Larkin et al., 2011, Brooks and Faulkner, 1988), and physiological cross-sectional areas (CSA) of the muscles were determined by dividing the mass of the muscle by the product of L_f and 1.06 g/cm^3, the density of mammalian skeletal muscle. The specific P_o was determined by dividing P_o by the physiological CSA.

Neuromuscular Junction (NMJ) imaging. For imaging acetylcholine receptors (AchRs), longitudinal muscle sections were permeabilized with 1% triton X-100 for 1 hour at room temperature and then incubated with Alexa Fluor 647-conjugated bungarotoxin (Molecular Probes, Eugene, OR, USA) diluted in PBS and 1% triton X-100 for one hour at room temperature. Sections were washed with PBS and mounted in Vectashield (Vector Laboratories, Peterborough, UK). Immune fluorescence imaging was obtained with a Nikon TE2000U microscope.

Analysis of fiber diameter, nuclei number and myonuclear domain. Gastrocnemius and quadriceps muscles were dissected, weighed and immediately placed in relaxing solution at 4^{o}C {0.1 M KCl, 0.01 M imidazole (pH 7.0), 1mM $MgCl_2$, 2 mM EGTA and 4.5 mM ATP}. The bundles of ≈ 50-100 fibers were dissected in the chilled relaxing solution and chemically skinned in relaxing solution containing 50% (v/v) glycerol for 24 h at 4^{o}C and stored at -20^{o}C for up to 4 weeks before use. On the day of the experiment, single fiber segments were gently dissected free from the bundle and carefully placed on the glass slide.

After a brief permeabilization with 0.1% Triton X-100, fibers were stained with rhodamine-phalloidin (1:200, Molecular Probe Inc., Eugene, OR, USA) for 45 minutes and DAPI (Invitrogen, Molecular Probes, OR, USA) for 5 minutes followed by final washes. Linear fiber segments of ≈350-450µm were chosen for imaging. All images were captured with a Nikon TE2000U inverted fluorescence microscope equipped with a 20 x phase-contrast objective (NA 0.45) and imported into Image J software (developed by Wayne Rasband, National Institute of Health, Bethesda, MD) for analysis.

MyHC isoforms composition by gel electrophoresis. In short, the myosin heavy chain (MyHC) isoform composition of the muscle was determined by SDS-PAGE as previously described (Larsson et al., 1993). The total acrylamide and *bis* concentration were 4% (w/v) in the stacking gel and 8% in the running gel, and the gel matrix included 30% glycerol. Sample loads were kept small to improve the resolution of the MyHC bands, and the electrophoresis was performed at 120 V for 24 h with a Tris-glycine electrode buffer (pH = 8.3) at 4°C.

Mitochondrial H_2O_2 generation. Intact isolated mitochondria from the gastrocnemius muscles were used to measure reactive oxygen species (ROS) generation indirectly as H_2O_2 release using the fluorescent probe Amplex Red (Molecular Probes, Eugene, OR, USA) as described previously (Muller et al., 2007, Zhang et al., 2013). The assay was performed in 100ul of reaction buffer that contained 125 mM KCl, 10 mM HEPES, 5 mM $MgCl_2$, and 2 mM K_2HPO_4 (pH 7.44) along 20-50 µg of mitochondrial protein with and without respiratory substrates GM (2.5 mM glutamate and 2.5 mM malate) at 37°C. Amplex Red oxidation by H_2O_2 every 2 s for ~10 min at an excitation of 545 nm and an emission of 590 nm was measured using a Fluoroskan-FL Ascent Type 374 multiwell plate reader (Labsystems, Helsinki, Finland).

Statistical analysis. Data are presented as mean ± SEM or SD for each experiment as detailed in the figure legends. Comparisons among the three groups were performed by analysis of variance (ANOVA) while Student's t-test was performed to compare 2 groups. Data were analyzed using SPSS 22 or Prism 6 and p values of less than 0.05 were considered statistically significant.

Results.

Generation and characterization of a conditional mouse model with reduced CuZnSOD targeted to neuronal tissue. NesCre x *Sod1*$^{flox/flox}$ mice (n*Sod1*KO mice) are expected to show a reduction in CuZnSOD expression in neuronal tissue with no change in CuZnSOD expression in other tissues (i.e., in muscle). As shown in Figure 1, n*Sod1*KO mice show a dramatic reduction in the activity (Figure 1A) and protein levels (Figure 1B) of CuZnSOD in brain and spinal cord. In contrast, CuZnSOD activity and level in gastrocnemius and quadriceps muscle from n*Sod1*KO mice are equivalent to the values measured in wild type mice. Thus, the n*Sod1*KO mice we have generated shows a neuron specific loss of CuZnSOD and normal levels of muscle CuZnSOD, giving us a model to test directly the role that reduced CuZnSOD in neurons plays in the loss of muscle mass and and NMJ disaggregation that is observed in *Sod1*KO mice.

Effect of neuronal depletion of CuZnSOD on muscle mass and strength. Our previous studies showed that *Sod1*KO mice have significant muscle atrophy in a number of muscles. For example, the mass of lower hind limb muscles, in particular the gastrocnemius muscle, a muscle that undergoes a significant loss of mass during aging (Muller et al., 2006, Larkin et al., 2011), is reduced by 30-45% by 20 months of age (Muller et al., 2006, Larkin et al., 2011, Jang et al., 2012). We have also reported that muscle strength, as measured by specific force, is reduced in *Sod1*KO mice approximately 50% at 8 month of age (Larkin et al., 2011). We measured muscle mass in a number of individual hind limb muscles in 17- to 20-month-old wild type and n*Sod1*KO mice. As shown in Figure 2A, mass was not altered in the gastrocnemius, tibialis anterior or extensor digitorum longus muscles, while quadriceps (~14%) and soleus muscles (less than 10%) showed small but significant reduction in mass. Muscle-specific effects were also evident in measures of contractile force (Figure 2B). Despite no change in mass, both the extensor digitorum longus and gastrocnemius showed small but significant reductions (~10%) in specific force. In contrast, the soleus muscle, which showed a reduction in mass, showed no loss of force generation.

Changes in muscle properties in gastrocnemius and quadriceps muscle from wild type and n*Sod1*KO mice. Because the gastrocnemius and quadriceps muscle showed differential changes in mass in response to the neuronal depletion of CuZnSOD, we measured a number of additional properties of these two muscles. We previously reported a significant reduction in fiber diameter in gastrocnemius muscle of 20-month-old *Sod1*KO mice compared to wild type mice as well as a reduction in the number of nuclei present per mm of muscle fiber (Jang et al., 2010) .The myonuclear domain (MND), which is a measure of the cytoplasmic domain per myonucleus, was not different in wild type and *Sod1*KO mice. We measured the fiber diameter in a total of 361 muscle fibers from gastrocnemius and quadriceps muscles of wild type

(N=5, n=225) and n*Sod1*KO (N=3, n=136) mice. In contrast to muscles of Sod1KO mice, the data in Figure 3A show there was no significant difference in fiber diameter between the two experimental groups in either muscle. We also measured the number of nuclei per mm of fiber length and calculated the size of the MNDs along the length of single muscle fiber linear segments. We found no difference in the number of nuclei per unit length between the wild type and nSod1KO mice in either muscle (Figure 3B). The MND was not altered in the gastrocnemius muscle, but was slightly reduced in fibers from the quadriceps muscle from n*Sod1*KO mice, reflecting a trend for a reduction in fiber size but unchanged nuclei count when compared to wild type muscle (Figure 3B). Both gastrocnemius and quadriceps muscle from n*Sod1*KO mice showed increased numbers of fibers with central nuclei (Figure 3C). This is in agreement with our previous finding of an increased numbers of central nuclei in gastrocnemius muscle from *Sod1*KO mice (Jang et al., 2012). The increase in central nuclei may suggest an increase in degeneration and regeneration of quadriceps muscle fibers in the n*Sod1*KO mice compared to wild type mice. Single muscle fiber size, force generation and the nuclei count vary between glycolytic and oxidative fibers and the changes described above can be influenced by the change in muscle fiber type composition. However, as shown in Figure 3D, we do not report a fiber type transition between gastrocnemius and quadriceps muscles from wild type and n*Sod1*KO mice.

Changes in NMJ morphology and markers of denervation. One of the most robust changes we have reported in the *Sod1*KO mice are changes NMJ structure and function and a loss of innervation and (Jang et al., 2010, Sakellariou et al., 2014, Shi et al., 2014). These same changes occur with age in wild type mice (Jang et al., 2012). To determine whether a selective loss of neuronal CuZnSOD can lead to alterations in NMJs and loss of innervation, we examined AChR morphology using immunostaining and quantified the changes in receptor endplate area. During aging, muscle atrophy is associated with fragmentation of AChRs, changes in shape and a reduction in receptor endplate area and we also observed these changes in muscle from the *Sod1*KO mice (Jang et al., 2012). As shown in Figure 4A, we found a significant reduction in endplate area in both gastrocnemius and quadriceps muscle from n*Sod1*KO mice compared to age matched wild type mice but no evidence of fragmentation. To determine if the n*Sod1*KO mice showed changes in innervation, we measured the induction of expression of acetylcholine receptor alpha (AChRα) and two other markers known to increase transiently in skeletal muscle following denervation, the transcription factors Runx1 and GADD45α (Figure 4B). The transcripts for these three genes were increased significantly in the gastrocnemius muscle from both *Sod1*KO and n*Sod1*KO mice compared to wild type mice. We found similar increases in these genes in quadriceps muscle from the nSod1K mice

(right panel in Figure 4B). However, the expression of two additional genes associated with the NMJ (MuSK and rapsyn) whose expression is increased with denervation, was not increased. These data suggest a morphological change in the AChR consistent with changes seen in the initiation of denervation; however, the NMJ fragmentation and denervation that occurs in muscle from the *Sod1*KO mice is not seen in the n*Sod1*KO mice.

Changes in mitochondrial function and oxidative damage. One of the most robust alterations we have measured in response to denervation is mitochondrial dysfunction, especially an increase in generation of H_2O_2 by isolated muscle mitochondria and increased oxidative damage. For example, we have reported dramatic increases in H_2O_2 in isolated muscle mitochondria from muscle after sciatic nerve transection and nerve crush (Muller et al., 2007, Walsh et al., 2015). Using the fluorescent probe Amplex Red, we measured H_2O_2 generation in mitochondria isolated from gastrocnemius of wild type and 17-22 month old n*Sod1*KO mice (Figure 5A). H_2O_2 generation was not significantly increased during State 1 respiration (no exogenous substrate provided) or in response to glutamate and malate as substrates in the gastrocnemius muscle of the n*Sod1*KO mice.

We have shown that the increased generation of ROS by mitochondria in the *Sod1*KO mice and other mouse models of denervation results in increased oxidative stress as measured by oxidative damage (Jang et al., 2010, Muller et al., 2007). To determine whether oxidative damage is elevated in muscle from n*Sod1*KO mice as we have previously reported in muscle from *Sod1*KO mice (Zhang et al., 2013b), we measured F_2-isoprostane levels, a marker of lipid peroxidation, in quadriceps muscle from wild type *Sod1*KO and n*Sod1*KO mice (Figure 5B). F_2-isoprostanes were elevated more than 30% in quadriceps muscle from *Sod1*KO mice compared to muscle from wild type mice, but were not elevated in muscle from the nSod1KO mice. Our previous studies show that loss of skeletal muscle mass in the *Sod1*KO mice is associated with increased oxidative damage and compensatory up-regulation of RONS regulatory enzymes (Sakellariou et al., 2011, Sakellariou et al., 2014). To determine whether protein nitration is increased in muscle from the n*Sod1*KO mice, we measured the levels of protein nitration (Figure 6A) and the protein content of PRXV (Figure 6B), a peroxynitrite reductase. No significant differences were observed in gastrocnemius muscle between wild type and n*Sod1*KO mice. To further assess muscle redox changes, we measured the expression of RONS regulatory enzymes including MnSOD, eNOS and iNOS (Figure 7). Similar to our results on protein nitration in the gastrocnemius, no significant difference in expression of RONS regulatory enzymes was detected in muscle tissue from n*Sod1*KO mice compared with wild type mice, indicating no change in the overall redox status in muscle of n*Sod1*KO mice.

Discussion.

Aging is accompanied by a 30% to 40% reduction in skeletal muscle mass and function that is the main cause of frailty and loss of independence in the elderly (Roubenoff and Hughes, 2000). This phenomenon, called sarcopenia, is universal to all mammalian species, and is observed even in the absence of disease. The loss of muscle mass involves both loss of muscle fibers and, to a lesser extent, atrophy of the remaining muscle fibers. Aging in skeletal muscle is associated with an increased number of fibers per motor unit and fiber type grouping consistent with a cycle of continual denervation and reinnervation (Essen-Gustavsson and Borges, 1986, Larsson and Edstrom, 1986). In addition to the changes that occur in muscle tissue, parallel changes have also been reported in motor neurons during aging that have been proposed to play an important role muscle atrophy, including loss of motor neurons and alterations in axonal sprouting (Fagg et al., 1981). While the etiology of sarcopenia is poorly understood, several potential contributing factors have been identified, including loss of innervation, muscle mitochondrial dysfunction, and oxidative stress (Fulle et al., 2004, Kadhiresan et al., 1996).

*Sod1*KO mice, lacking CuZnSOD in all tissues, have elevated levels of oxidative damage and a significantly shortened lifespan (30% reduction) compared to wild type mice (Zhang et al., 2013, Elchuri et al., 2005). The lifespan of the *Sod1*KO mice can be restored to that of wild type mice by dietary restriction (Zhang et al., 2013b). In addition, many aging phenotypes are accelerated in the Sod1KO mice, e.g., loss of hearing and hair, thinning of skin, cataracts, and early onset of muscle atrophy (Muller et al., 2006, Elchuri et al., 2005, McFadden et al., 1999). The accelerated loss of muscle in the *Sod1*KO mice is similar in essentially every respect to the sarcopenia observed with aging in wild type mice (Jang et al., 2011). These similarities include an age-dependent decrease in muscle mass (both absolute and relative to body mass) with the greatest decrease occurring in the gastrocnemius, with the greatest decrease occurring in the gastrocnemius, a muscle profoundly affected by aging in wild type mice; a higher percentage of smaller muscle fibers, evident even in adult (8 month old) Sod1KO mice; and a failed adaptive response (Visilaki et al., 2010). The reduction in muscle mass is 30% to 45% in hind limb muscle mass in *Sod1KO* mice by 20 months of age whereas wild type mice show little change in hind limb muscle mass until after 26 months of age (Muller et al., 2006). The accelerated loss of muscle mass is associated with neuronal changes, again, similar to those described in old wild type mice. These include the loss of functional innervation (Larkin et al., 2011)) with gross alterations in NMJ morphology, including reduced occupancy of the motor endplates by axons, terminal sprouting, axon thinning, and irregular swelling with reduced motor neuron myelin thickness and fiber/axon diameter (Muller et al., 2006, Shi et al., 2014, Hamilton et al., 2013). The decrease in muscle mass and function and changes in neuronal structure and

function are prevented in both adult *Sod1*KO and old wild type mice subjected to dietary restriction (Jang et al., 2012, Zhang et al.,2013b).

Using transgenic and knockout mouse models that conditionally express CuZnSOD, we have begun to define the role muscle and motor neurons play in the accelerated loss of muscle observed in the *Sod1*KO mice. Our previous studies showed that (1) *Sod1*KO mice expressing CuZnSOD specifically in neuronal tissue (nSOD1-Tg/*Sod1*KO mice) were protected from the muscle atrophy and weakness as well as from the NMJ degeneration (Sakellariou et al., 2014) and (2) m*Sod1*KO mice, in which *Sod1* is deleted specifically in skeletal muscle, showed no muscle atrophy or NMJ degeneration (Zhang et al., 2013a). Based on the observation that the loss of CuZnSOD in muscle appeared to have very little effect on muscle atrophy, we proposed that the accelerated sarcopenia phenotype we observed in the *Sod1*KO mice occurred as a result of increased oxidative stress in the motor neurons, which led to NMJ dysfunction/disaggregation and the eventual loss of muscle mass and function, Thus, we predicted that deletion of CuZnSOD in neuronal tissue (in the n*Sod1*KO mice) would recapitulate the sarcopenia phenotype observed in the *Sod1*KO mice. However, our data show that the mass of the gastrocnemius, which is the muscle showing the greatest atrophy in *Sod1*KO and old wild type mice, was not reduced in n*Sod1*KO compared to wild type mice, even at 20 months of age. In addition, no reduction in mass of the tibialis anterior and extensor digitorum longus muscles was observed in the n*Sod*1KO mice. At 20-25 months of age, the *Sod1*KO mice show over a 50% decrease in the muscle mass of the gastrocnemius and a 19% to 25% decrease in the mass of the tibialis anterior and extensor digitorum longus muscles. We did observe a slight but significant decrease in the mass of the quadriceps and soleus muscles in the n*Sod1*KO mice, which was similar to the decrease observed in *Sod1*KO mice. Interestingly, the data from the m*Sod1*KO and n*Sod1*KO mice show that changes in muscle force generation and muscle mass appear to occur through separate mechanisms because muscle atrophy (quantity) and muscle weakness (quality) did not always parallel each other. For example, gastrocnemius muscles of m*Sod1*KO mice were weaker than those of wild type, as indicated by lower values for specific force (normalized for muscle cross-sectional area) even though the mass of the gastrocnemius muscles of the m*Sod1*KO mice was slightly larger (nearly a 15-20% increase in mass relative to body weight in m*Sod1*KO versus wild type mice). I n the present study, we observed that the gastrocnemius and the extensor digitorum longus muscles from the n*Sod1*KO mice were also significantly weaker than those of WT mice even though the masses of the muscles were not different between the nSod1KO and WT mice. On the other hand, the soleus showed a decrease in muscle mass in the n*Sod1*KO mice and a concomitant decrease in absolute force, but specific force was not different between n*Sod1*KO and WT mice, indicating no qualitative

change in the force generating capacity of the tissue.

In contrast to the m*Sod1*KO mice, we found that the n*Sod1*KO mice at 17-22 months of age showed changes in NMJ morphology (reduced endplate area) and increased expression of AChRa, Runx1 and gadd45a, genes associated with denervation (Jang et al., 2010, Wang et al., 2005, Bongers et al., 2013). However, we did not observe any evidence of NMJ fragmentation in the n*Sod1*KO mice. In contrast, *Sod1*KO mice show evidence of NMJ fragmentation as early as 5 months of age (Jang et al., 2012). These results suggest that deleting *Sod1* in neuronal tissue has an effect on NMJ structure/function; however, this effect is much less severe than that which occurs in the *Sod1*KO mouse. We have found the induction of production of reactive oxygen species by isolated muscle mitochondrial (mtROS, as measured by H_2O_2 generation) and increased oxidative damage and stress in muscle to be consistently associated with NMJ fragmentation and denervation. For example, mtROS is induced over 30-fold following sciatic nerve transection (Muller et al, 2007). In addition, the level of mtROS production by muscle is correlated with the severity of muscle atrophy [e.g, mtROS increased approximately 30% in 30-month-old wild type mice, more than 50% in 20-month-old *Sod1*KO mice, and approximately 75% in muscle from symptomatic amyotrophic lateral sclerosis (ALS) mice (Muller et al, 2007) and dietary restriction dramatically reduces muscle atrophy and mtROS generation in muscle of the *Sod1*KO mice (Jang et al., 2012). We did not observe any significant change in either mtROS generation, oxidative damage (measured by F_2-isoprostane or protein nitration levels), or oxidative stress (measured by RONS regulatory enzymes) in the muscle of the n*Sod1*KO mice. Thus, the changes we observed in the NMJs of the n*Sod1*KO mice do not lead to changes in the muscle that we observe in the *Sod1*KO mice.

Based on our data with the conditional knockout and transgenic mice, we propose that muscle atrophy in *Sod1*KO mice occurs through a "two-hit" mechanism involving changes in motor neurons and changes in muscle. We propose that the "first hit" occurs when redox homeostasis is compromised in motor neurons resulting in alteration in NMJ morphology and function. The "second hit" occurs when the muscle mitochondria are altered (e.g., increased ROS production) in response to NMJ dysfunction and the alteration in muscle mitochondria triggers a retrograde response leading to increased NMJ damage, which in turn leads to further dysfunction in NMJs and motor neurons. The increased NMJ dysfunction leads to a further increase in muscle mitochondrial dysfunction, resulting in a vicious cycle that ultimately results in NMJ fragmentation, denervation, loss of muscle fibers, and sarcopenia. Preventing the initial motor neuron defect, as in the nSOD1-Tg/*Sod1*KO mouse, prevents the mitochondria dysfunction and increased oxidative damage/stress in muscle as well as the cascade of events leading to sarcopenia even though the antioxidant defense system in the muscle is compromised.

The m*Sod1*KO mice, which show no NMJ fragmentation, mitochondria dysfunction, or oxidative damage/stress support the “two-hit” mechanism by showing that without the initial motor neuron dysfunction there is no trigger to induce mitochondria dysfunction in muscle mitochondria and therefore, no NMJ fragmentation, again indicating that the dysfunction in motor neurons/NMJ is necessary to initiate the mitochondria dysfunction in the muscle. Finally, n*Sod1*KO mice do not show muscle atrophy in most muscles because the initial motor neuron dysfunction does not trigger sufficient mitochondrial dysfunction and oxidative damage/stress in the muscle of the n*Sod1*KO mice, which have an intact antioxidant defense system. Therefore, the n*Sod1*KO mice lack the “second hit,” which would lead to the vicious cycle and increased NMJ dysfunction and fragmentation.

Acknowledgments.

This work was support by a grant from the NIH/NIA to Drs. Brooks, Jackson, McArdle, Richardson and Van Remmen (P01 AG020591) and a VA Merit grant to HVR. The authors would also like to thank Dr. Wenbo Qi for his assistance with the assay of F_2-isoprotanes levels.

Figure legends

Figure 1: Generation of neuron-specific Sod1-knockout (n*Sod1*KO) mice. A) Native gels stained for CuZnSOD and MnSOD enzyme activities in gastrocnemius, quadriceps, brain and spinal cord of wild type and n*Sod1*KO mice. B) Western blot analysis of CuZnSOD expression in gastrocnemius, quadriceps, brain and spinal cord of wild type and n*Sod1*KO. (n=3-6 mice in each group between 7 and 18 months of age). Both males and females were used to generate these data.

Figure 2: Muscle mass and function of the nSOD1KO mice. A) Muscle mass expressed as percentage of body mass. B) Maximum isometric specific force (N/cm^2) of gastrocnemius, extensor digitorum longus and soleus muscle. (*p<0.05 vs wild type by Students t-test, n=8-10 mice per group, 20 month old mice, wild type -black bars, n*Sod1*KO- white bars)

Figure 3: Fiber diameter, type, myonuclear domain (MND) and number of nuclei in gastrocnemius and quadriceps muscle of the n*SOD1*KO mice. A) Percentage distribution of fiber diameter of gastrocnemius and quadriceps muscle. B) MND size from single muscle fiber segments of gastrocnemius and quadriceps. Rhodamine-phalloidin labeled actin is shown in red and nuclei visualized by DAPI in blue. Scale bar denotes 50μm. C) Fibers with central nuclei in the gastrocnemius and quadriceps. D) Percentage of fiber type distribution in the gastrocnemius and quadriceps (*p=0.05 vs wild type by t-test, n= 3-7 mice in each group). 5 months and 20 months old mice were used.

Figure 4: Acetylcholine receptor morphology and denervation associated markers in n*Sod1*KO mice A). Acetylcholine receptors from gastrocnemius (GTN) (A, B, C, D) and quadriceps (Quad) muscles (E, F, G, H). (scale bar = 10mm for receptors and 40mm for clusters). B). mRNA levels of the denervation markers. In gastrocnemius,*p<0.001 nSod1KO vs wild type, *p<0.01 Sod1KO vs wild type for AChRα mRNA; *p<0.01 nSod1KO vs wild type, *p<0.0001 Sod1KO vs wild type for Runx1 mRNA;*p<0.05 nSod1KO vs wild type, *p<0.001 Sod1KO vs wild type for GADD45α mRNA by analysis of variance (ANOVA) with comparisons between groups performed using Newman-Keuls post –hoc test using Prism6 software. In quadriceps,*p<0.01 nSod1KO vs WT for AChRα mRNA; *p<0.0001 nSod1KO vs WT for Runx1 mRNA,*p<0.05 nSod1KO vs wild type for GADD45a mRNA by t-test. Mice were 16-18months of age and n= 4-13 mice per group. (WT -black bars, n*Sod1*KO- white bars, *Sod1*KO- grey bars).

Figure 5: Mitochondrial ROS measurement and F_2-isoprostane levels in n*Sod1*KO mice A) Hydrogen peroxide generation in mitochondria isolated from gastrocnemius muscle (n= 6-11 mice per group). B) F_2-isoprostane levels in quadriceps muscle (*p< 0.05 in wild type vs Sod1KO by Students t test; n= 3-5 mice

per group) (wild type -black bars, *Sod1*KO – grey bars, n*Sod1*KO- white bars).

Figure 6: Markers of oxidative damage to proteins in nSOD1KO mice. A) Protein nitration in gastrocnemius and quadriceps. B) Expression of peroxynitrite reductase, PRXV in the gastrocnemius and quadriceps. (n=4 mice per group, 17-22 month old mice with quantification on the right) (wild type- black bars, nSOD1KO- white bars).

Figure 7: RONS regulatory protein contents in nSOD1KO mice. Expression of MnSOD, endothelial nitric oxide synthase (eNOS) and inducible NOS (iNOS) proteins of gastrocnemius and quadriceps by western blot with quantification on the right. (n=4mice per group, 17-22 month old mice) (wild type -black bars, nSOD1KO- white bars).

References

Bongers, K.S., Fox, D.K., Ebert, S.M., Kunkel, S.D., Dyle, M.C., Bullard, S.A., Dierdorff, J.M., and Adams, C.M. (2013). Skeletal muscle denervation causes skeletal muscle atrophy through a pathway that involves both Gadd45a and HDAC4. American journal of physiology. Endocrinology and Metabolism *305*, E907-915.

Brooks, S.V., and Faulkner, J.A. (1988). Contractile properties of skeletal muscles from young, adult and aged mice. J Physiol *404*, 71-82.

Elchuri, S., Oberley, T.D., Qi, W., Eisenstein, R.S., Jackson Roberts, L., Van Remmen, H., Epstein, C.J., and Huang, T.T. (2005). CuZnSOD deficiency leads to persistent and widespread oxidative damage and hepatocarcinogenesis later in life. Oncogene *24*, 367-380.

Essen-Gustavsson, B., and Borges, O. (1986). Histochemical and metabolic characteristics of human skeletal muscle in relation to age. Acta Physiol Scand *126*, 107-114.

Fagg, G.E., Scheff, S.W., and Cotman, C.W. (1981). Axonal sprouting at the neuromuscular junction of adult and aged rats. Exp Neurol *74*, 847-854.

Fulle, S., Protasi, F., Di Tano, G., Pietrangelo, T., Beltramin, A., Boncompagni, S., Vecchiet, L., and Fano, G. (2004). The contribution of reactive oxygen species to sarcopenia and muscle ageing. Exp Gerontol *39*, 17-24.

Hamilton, R.T., Bhattacharya, A., Walsh, M.E., Shi, Y., Wei, R., Zhang, Y., Rodriguez, K.A., Buffenstein, R., Chaudhuri, A.R., and Van Remmen, H. (2013). Elevated protein carbonylation, and misfolding in sciatic nerve from db/db and Sod1(-/-) mice: plausible link between oxidative stress and demyelination. PLoS One *8*, e65725.

Jang, Y.C., Lustgarten, M.S., Liu, Y.H., Muller, F.L., Bhattacharya, A., Liang, H.Y., Salmon, A.B., Brooks, S.V., Larkin, L., Hayworth, C.R., et al. (2010). Increased superoxide in vivo accelerates age-associated muscle atrophy through mitochondrial dysfunction and neuromuscular junction degeneration. FASEB J *24*, 1376-1390.

Jang, Y.C., and Van Remmen, H. (2011). Age-associated alterations of the neuromuscular junction. Exp Gerontol *46*, 193-198.

Jang, Y.C., Liu, Y., Hayworth, C.R., Bhattacharya, A., Lustgarten, M.S., Muller, F.L., Chaudhuri, A., Qi, W., Li, Y., Huang, J.Y., et al. (2012). Dietary restriction attenuates age-associated muscle atrophy by lowering oxidative stress in mice even in complete absence of CuZnSOD. Aging Cell *11*, 770-782.

Kadhiresan, V.A., Hassett, C.A., and Faulkner, J.A. (1996). Properties of single motor units in medial gastrocnemius muscles of adult and old rats. J Physiol *493 (Pt 2)*, 543-552.

Larkin, L.M., Davis, C.S., Sims-Robinson, C., Kostrominova, T.Y., Van Remmen, H., Richardson, A., Feldman, E.L., and Brooks, S.V. (2011). Skeletal muscle weakness due to deficiency of CuZn-superoxide dismutase is associated with loss of functional innervation. Am J Physiol Regul Integr Comp Physiol *301*, R1400-1407.

Larsson, L., and Edstrom, L. (1986). Effects of age on enzyme-histochemical fibre spectra and contractile properties of fast- and slow-twitch skeletal muscles in the rat. J Neurol Sci *76*, 69-89.Larsson L and Moss

R. L. (1993). Maximum velocity of shortening in relation to myosin isoform composition in single fibers from human skeletal muscles. J Physiol 472, 595-614

McFadden, S.L., Ding, D., Burkard, R.F., Jiang, H., Reaume, A.G., Flood, D.G., and Salvi, R.J. (1999). Cu/Zn SOD deficiency potentiates hearing loss and cochlear pathology in aged 129,mCD-1 mice. The Journal of comparative neurology *413*, 101-112.

Muller, F.L., Song, W., Liu, Y., Chaudhuri, A., Pieke-Dahl, S., Strong, R., Huang, T.T., Epstein, C.J., Roberts, L.J., 2nd, Csete, M., et al. (2006). Absence of CuZn superoxide dismutase leads to elevated oxidative stress and acceleration of age-dependent skeletal muscle atrophy. Free Radic Biol Med *40*, 1993-2004.

Muller, F.L., Song, W., Jang, Y.C., Liu, Y., Sabia, M., Richardson, A., and Van Remmen, H. (2007). Denervation-induced skeletal muscle atrophy is associated with increased mitochondrial ROS production. Am J Physiol-Reg I *293*, R1159-R1168.

Roubenoff, R., and Hughes, V.A. (2000). Sarcopenia: current concepts. J Gerontol A Biol Sci Med Sci *55*, M716-724.

Sakellariou, G.K., Pye, D., Vasilaki, A., Zibrik, L., Palomero, J., Kabayo, T., McArdle, F., Van Remmen, H., Richardson, A., Tidball, J.G., et al. (2011). Role of superoxide-nitric oxide interactions in the accelerated age-related loss of muscle mass in mice lacking Cu,Zn superoxide dismutase. Aging Cell *10*, 749-760.

Sakellariou, G.K., Davis, C.S., Shi, Y., Ivannikov, M.V., Zhang, Y., Vasilaki, A., Macleod, G.T., Richardson, A., Van Remmen, H., Jackson, M.J., et al. (2014). Neuron-specific expression of CuZnSOD prevents the loss of muscle mass and function that occurs in homozygous CuZnSOD-knockout mice. FASEB J.

Shi, Y., Ivannikov, M.V., Walsh, M.E., Liu, Y., Zhang, Y., Jaramillo, C.A., Macleod, G.T., and Van Remmen, H. (2014). The lack of CuZnSOD leads to impaired neurotransmitter release, neuromuscular junction destabilization and reduced muscle strength in mice. PLoS One *9*, e100834.

Van Remmen, H., Salvador, C., Yang, H., Huang, T.T., Epstein, C.J., and Richardson, A. (1999). Characterization of the antioxidant status of the heterozygous manganese superoxide dismutase knockout mouse. Arch Biochem Biophys *363*, 91-97.

Vasilaki, A., van der Meulen, J.H., Larkin, L., Harrison, D.C., Pearson, T., Van Remmen, H., Richardson, A., Brooks, S.V., Jackson, M.J., and McArdle, A. (2010). The age-related failure of adaptive responses to contractile activity in skeletal muscle is mimicked in young mice by deletion of Cu,Zn superoxide dismutase. Aging Cell *9*, 979-990.

Walsh, M.E., Bhattacharya, A., Liu, Y., and Van Remmen, H. (2015). Butyrate prevents muscle atrophy after sciatic nerve crush. Muscle & nerve. *In Press*

Wang, X., Blagden, C., Fan, J., Nowak, S.J., Taniuchi, I., Littman, D.R., and Burden, S.J. (2005). Runx1 prevents wasting, myofibrillar disorganization, and autophagy of skeletal muscle. Genes & development *19*, 1715-1722.

Ward, W.F., Qi, W., Van Remmen, H., Zackert, W.E., Roberts, L.J., 2nd, and Richardson, A. (2005). Effects of age and caloric restriction on lipid peroxidation: measurement of oxidative stress by F2-isoprostane levels. J Gerontol A Biol Sci Med Sci *60*, 847-851.

Zhang, Y., Davis, C., Sakellariou, G.K., Shi, Y., Kayani, A.C., Pulliam, D., Bhattacharya, A., Richardson, A., Jackson, M.J., McArdle, A., et al. (2013a). CuZnSOD gene deletion targeted to skeletal muscle leads to loss of contractile force but does not cause muscle atrophy in adult mice. FASEB J *27*, 3536-3548.

Zhang, Y., Ikeno, Y., Bokov, A., Gelfond, J., Jaramillo, C., Zhang, H.M., Liu, Y., Qi, W., Hubbard, G., Richardson, A., et al. (2013b). Dietary restriction attenuates the accelerated aging phenotype of Sod1-/- mice. Free Radical Biology and Medicine *60*, 300-306.

Graphical Abstract

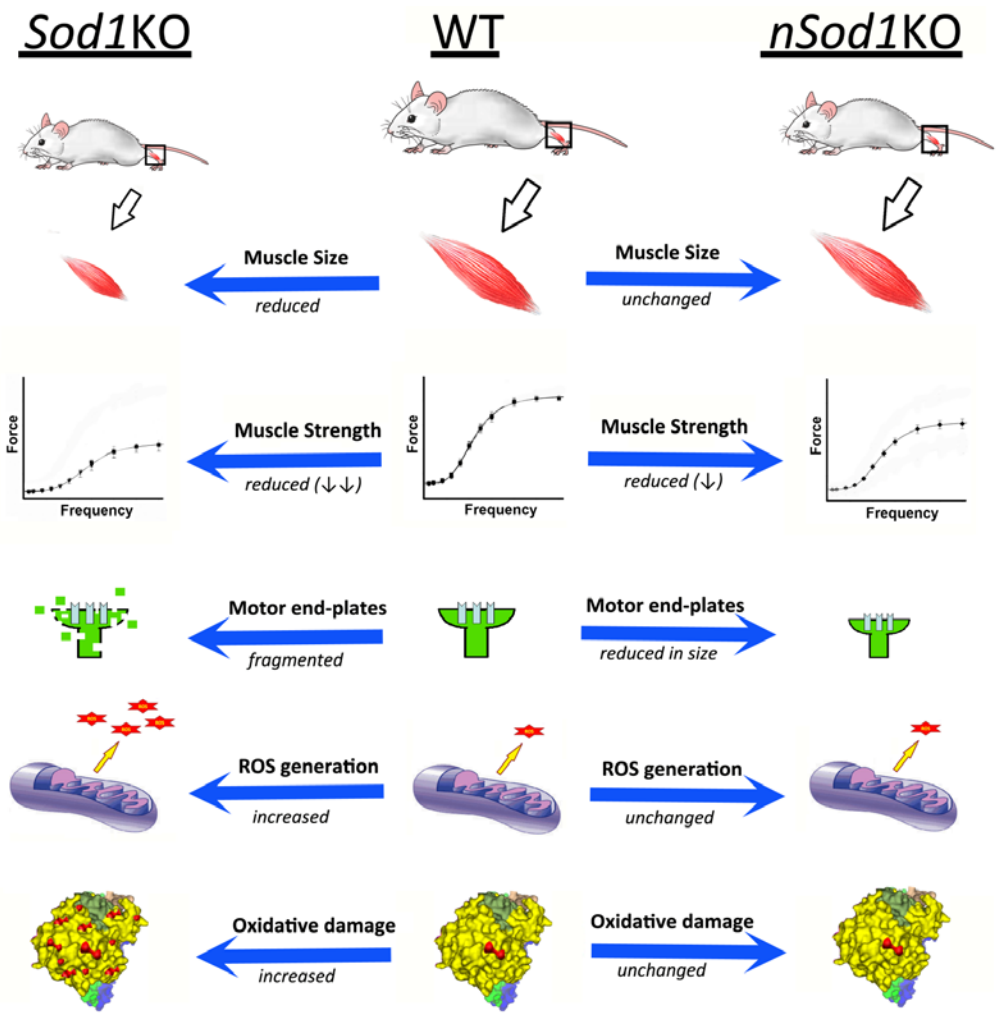

Figure 1

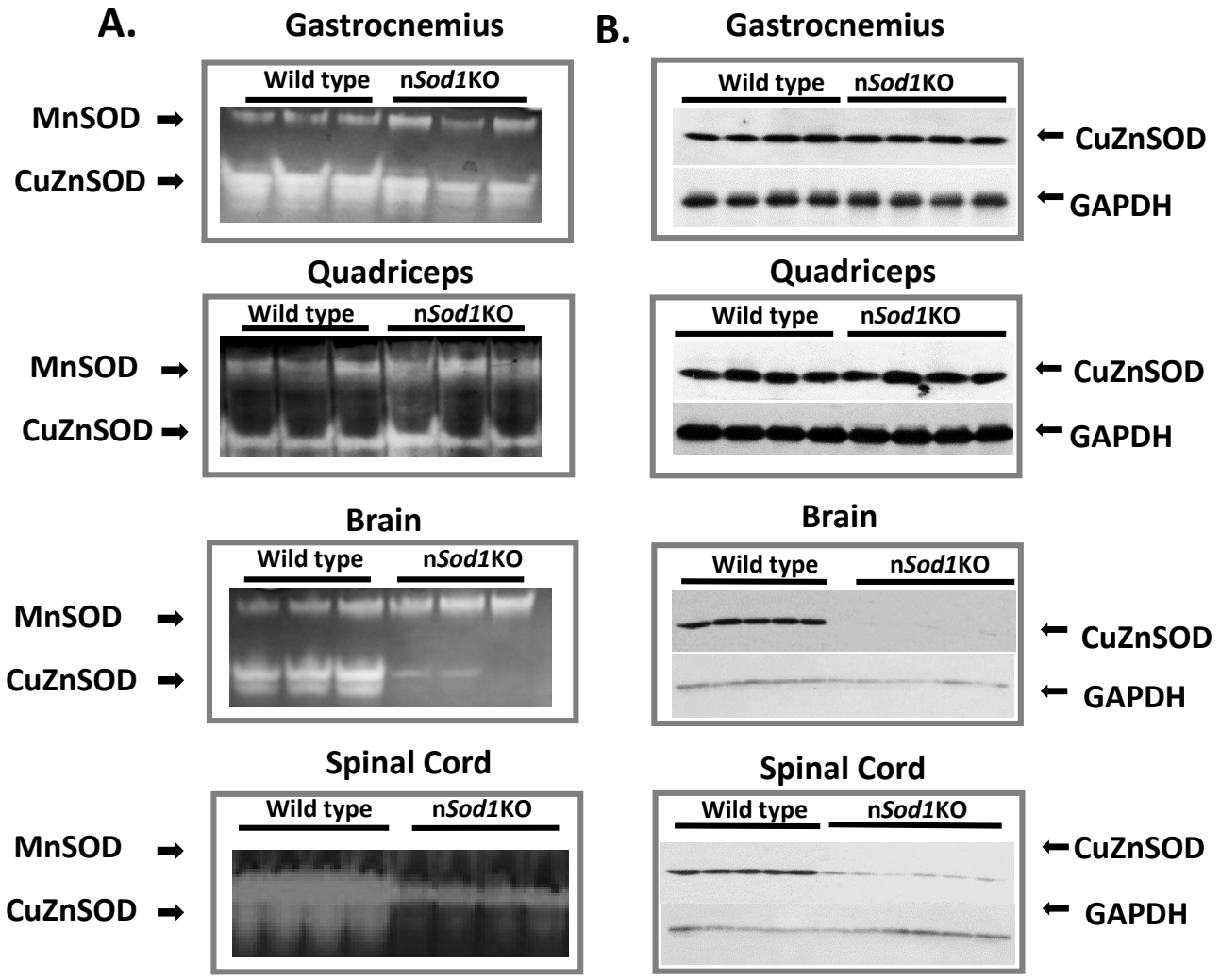
A.
Gastrocnemius
Wild type
nSod1KO
MnSOD
CuZnSOD
Quadriceps
Brain
Spinal Cord
B.
Gastrocnemius
CuZnSOD
GAPDH
Quadriceps
Brain
Spinal Cord

Figure 2

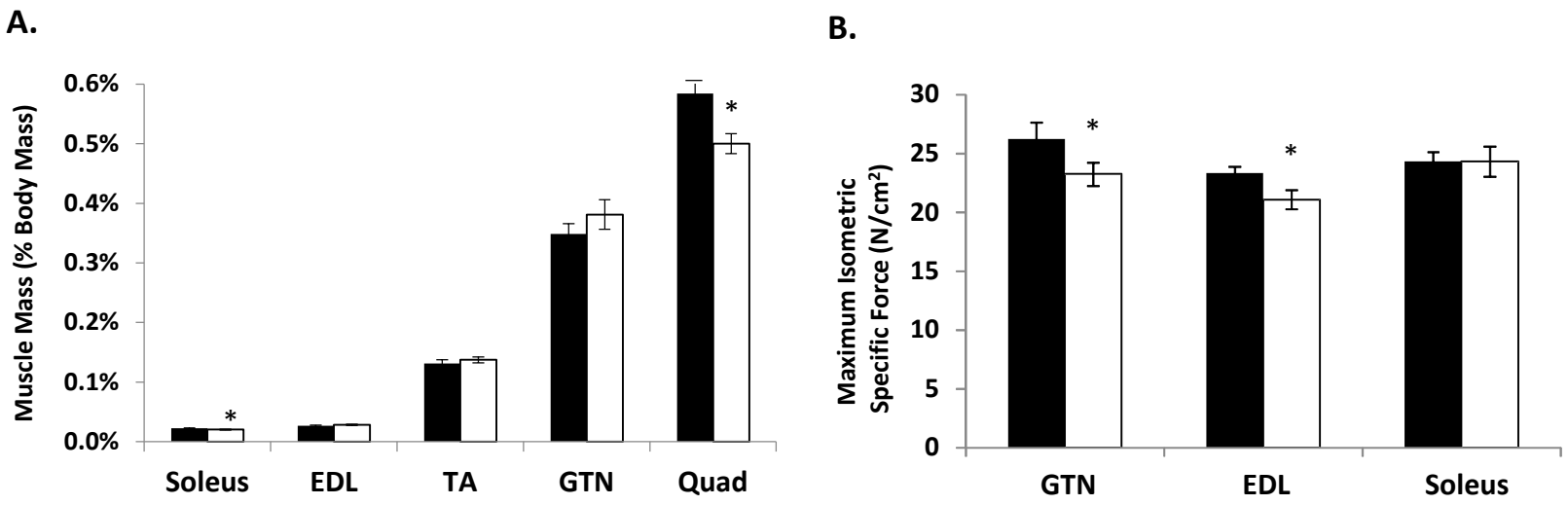
A.
Muscle Mass (% Body Mass)
0.6%
0.5%
0.4%
0.3%
0.2%
0.1%
0.0%
*
*
Soleus
EDL
TA
GTN
Quad
B.
Maximum Isometric Specific Force (N/cm²)
30
25
20
15
10
5
0
*
*
GTN
EDL
Soleus

Figure 3

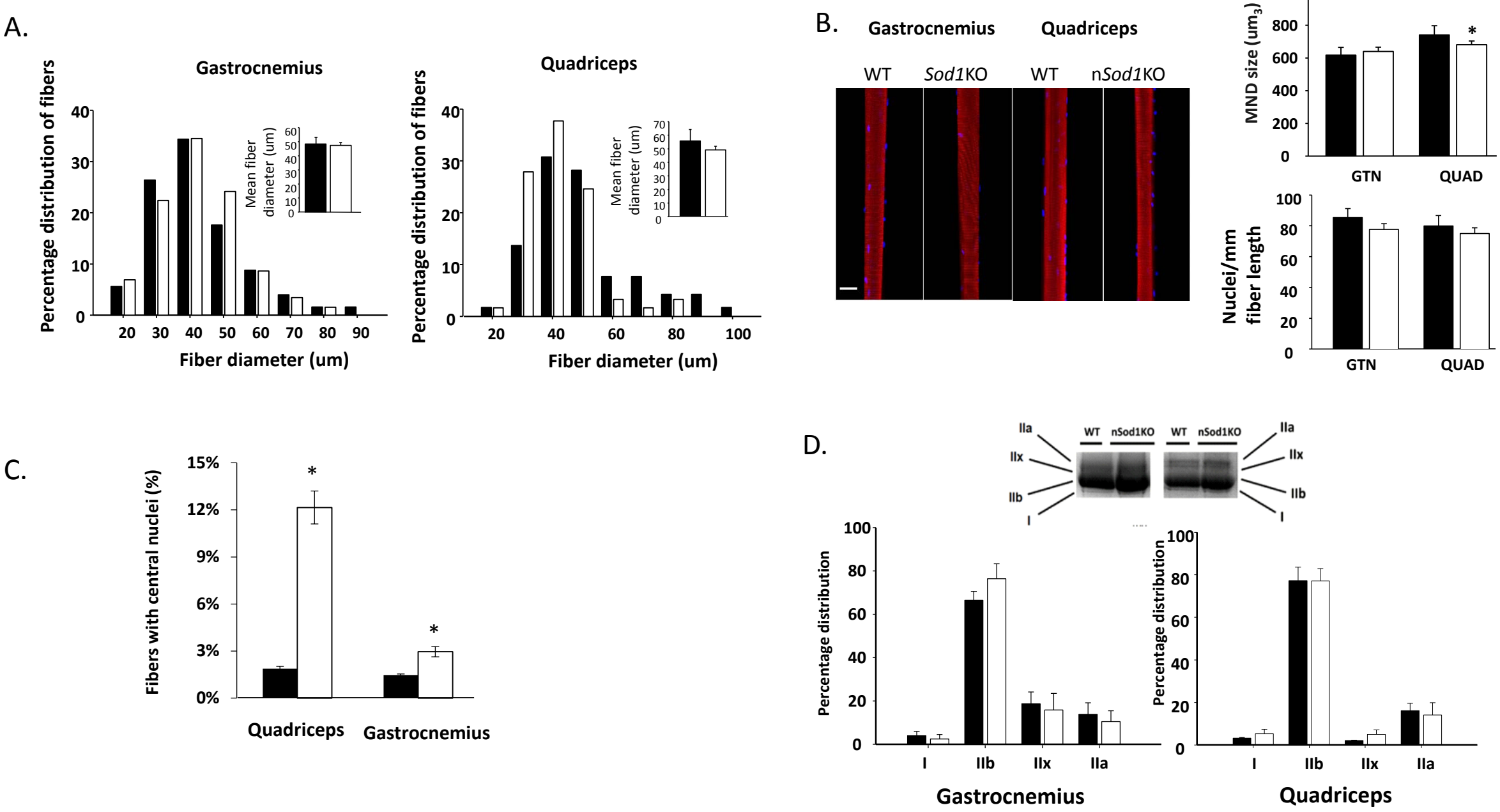
A.
Gastrocnemius
Quadriceps
Percentage distribution of fibers
Fiber diameter (um)
Mean fiber diameter (um)
B.
Gastrocnemius
Quadriceps
WT
Sod1KO
WT
nSod1KO
MND size (um3)
GTN
QUAD
Nuclei/mm fiber length
C.
Fibers with central nuclei (%)
Quadriceps
Gastrocnemius
D.
IIa
IIx
IIb
I
WT
nSod1KO
Percentage distribution
Gastrocnemius
Quadriceps

Figure 4

A.

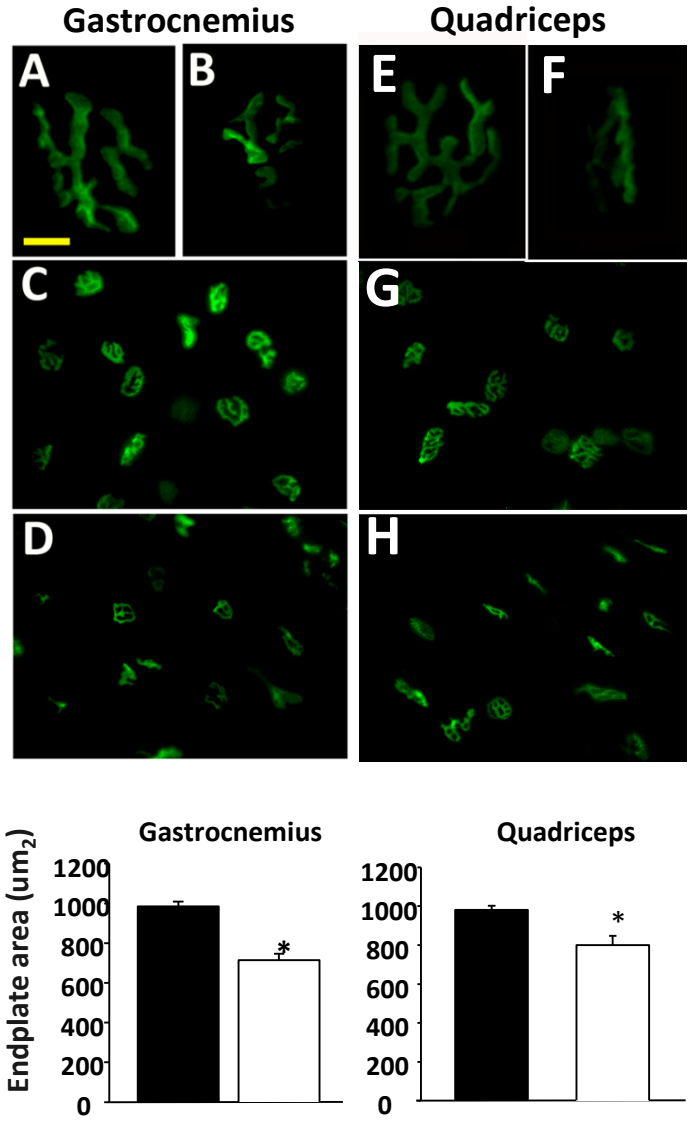
Gastrocnemius
Quadriceps
A
B
E
F
C
G
D
H
Gastrocnemius
Quadriceps
Endplate area (um2)
1200
1000
800
600
400
200
0
*
*

B.

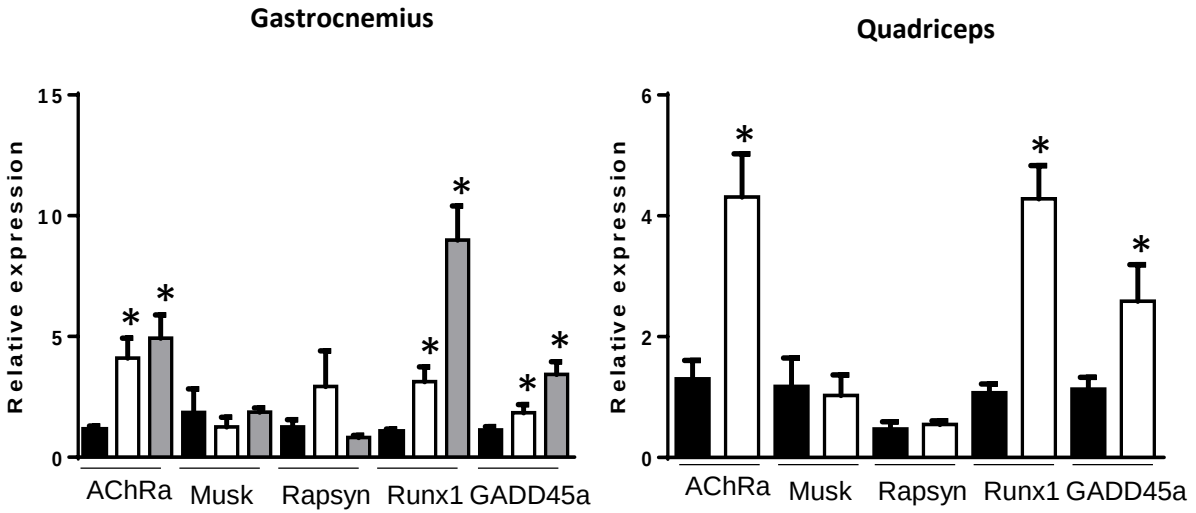
Gastrocnemius
Quadriceps
Relative expression
15
10
5
0
6
4
2
0
*
AChRa
Musk
Rapsyn
Runx1
GADD45a

Figure 5.

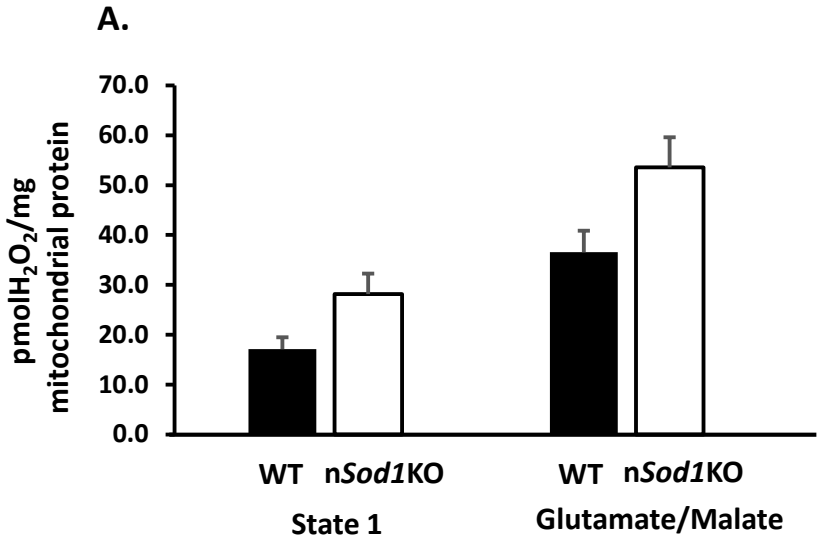
A.
pmolH2O2/mg mitochondrial protein
70.0
60.0
50.0
40.0
30.0
20.0
10.0
0.0
WT
nSod1KO
WT
nSod1KO
State 1
Glutamate/Malate

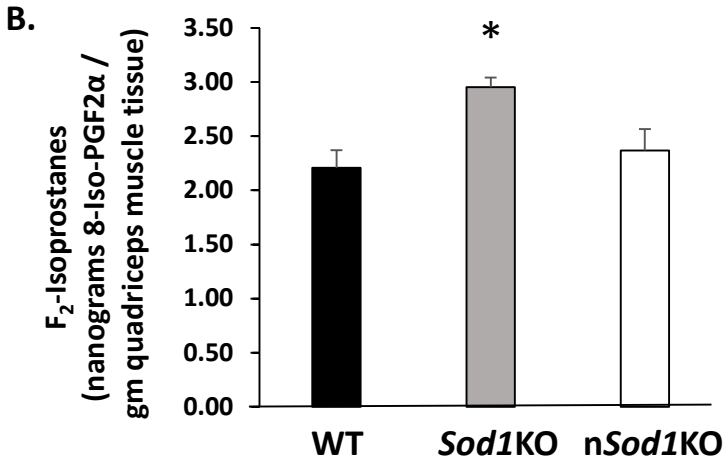
B.
F2-Isoprostanes (nanograms 8-Iso-PGF2α / gm quadriceps muscle tissue)
3.50
3.00
2.50
2.00
1.50
1.00
0.50
0.00
*
WT
Sod1KO
nSod1KO

Figure 6

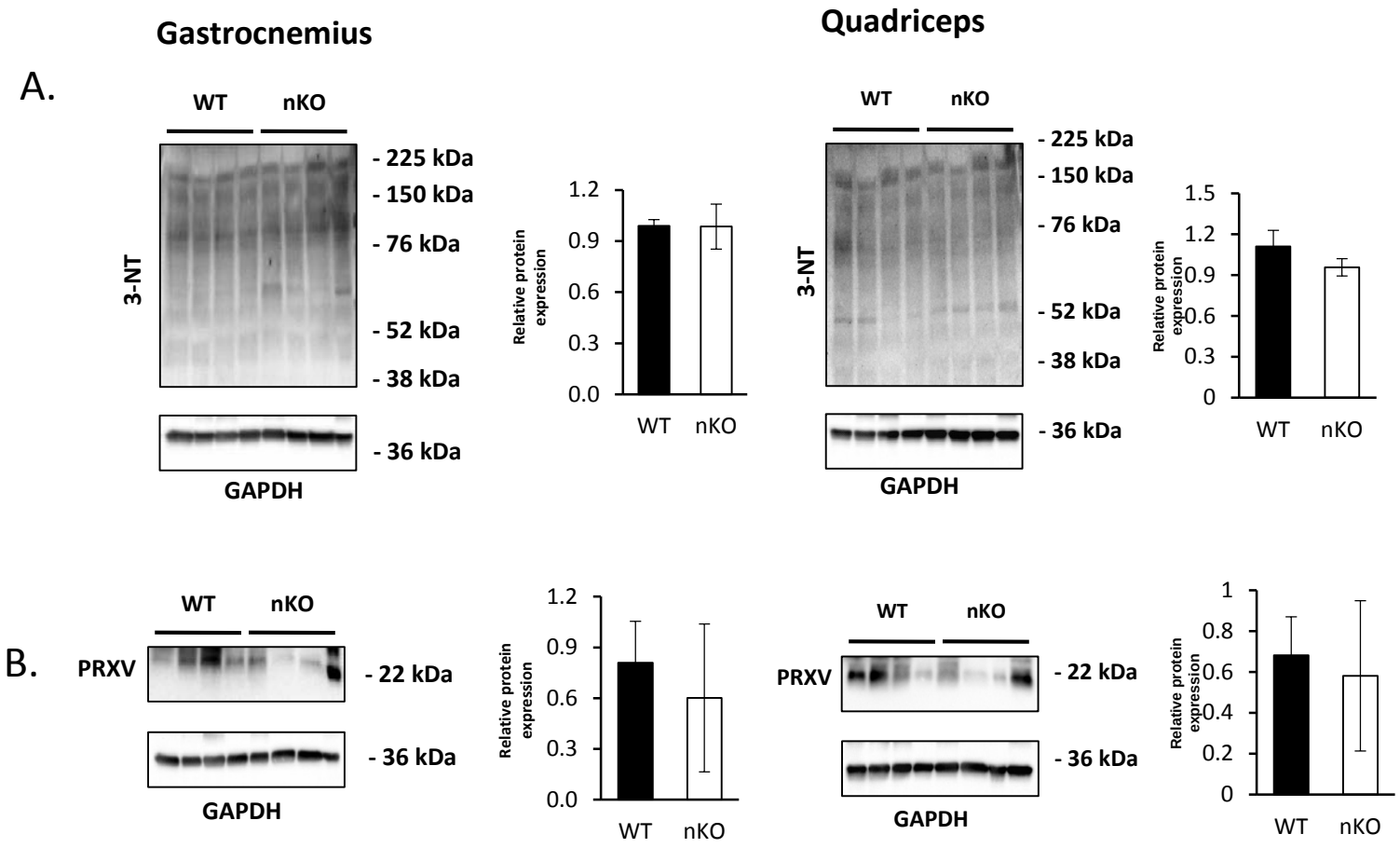
Gastrocnemius
Quadriceps
A.
WT
nKO
3-NT
- 225 kDa
- 150 kDa
- 76 kDa
- 52 kDa
- 38 kDa
- 36 kDa
GAPDH
Relative protein expression
1.2
0.9
0.6
0.3
0.0
1.5
1.2
0.9
0.6
0.3
0
WT
nKO
B.
PRXV
- 22 kDa
- 36 kDa
GAPDH
1
0.8
0.6
0.4
0.2
0

Figure 7

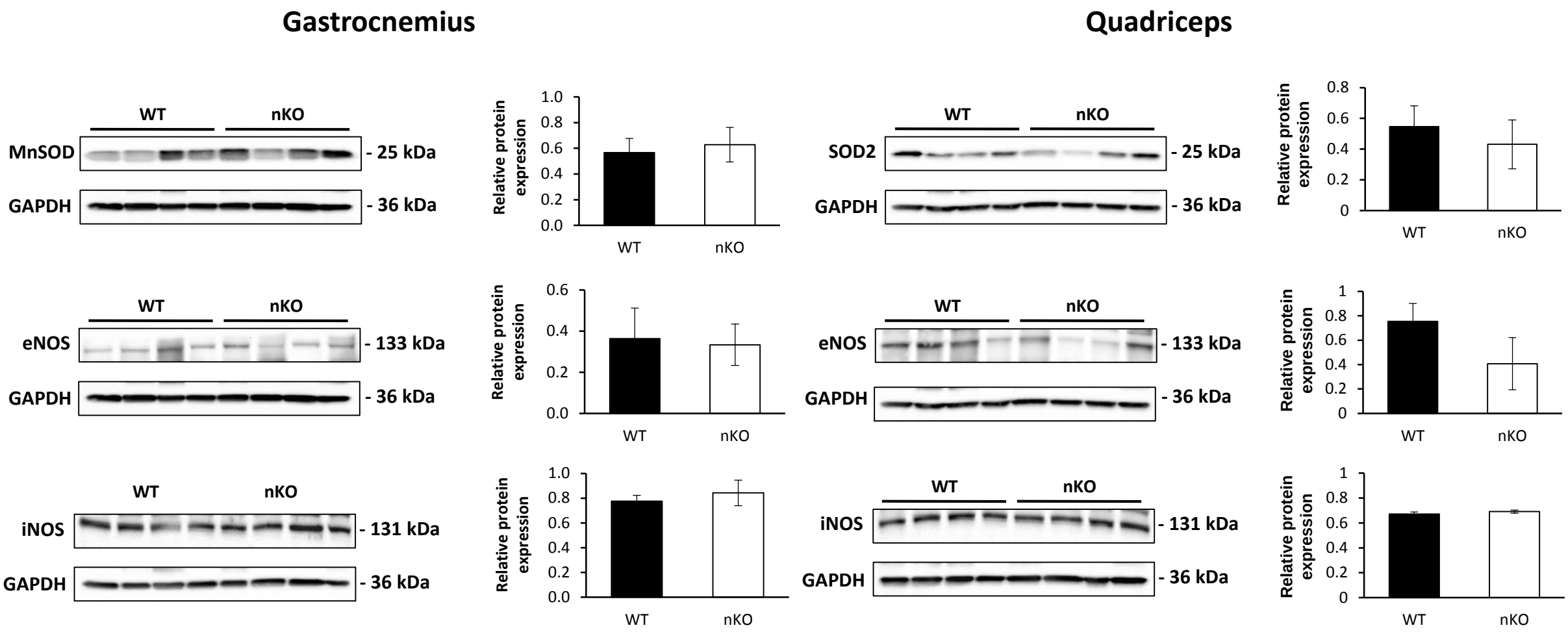
Gastrocnemius
Quadriceps
WT
nKO
MnSOD
- 25 kDa
GAPDH
- 36 kDa
SOD2
- 25 kDa
GAPDH
- 36 kDa
Relative protein expression
1.0
0.8
0.6
0.4
0.2
0.0
WT
nKO
0.8
0.6
0.4
0.2
0
eNOS
- 133 kDa
GAPDH
- 36 kDa
0.6
0.4
0.2
0.0
1
0.8
0.6
0.4
0.2
0
iNOS
- 131 kDa
GAPDH
- 36 kDa
1.0
0.8
0.6
0.4
0.2
0.0
1
0.8
0.6
0.4
0.2
0